

# Doping effect of sulfur substituting on Zirconium dioxide ZrO<sub>2</sub>

Samira Idrissi<sup>1</sup>, soumia ziti<sup>2</sup>, labrim hicham<sup>3</sup>, and Bahmad Lahoucine<sup>4</sup>

<sup>1</sup>Mohammed V University of Rabat

<sup>2</sup>Intelligence Artificial and Security of Systems, Mohammed V University of Rabat, Faculty of Sciences, B.P. 1014 Rabat, Morocco.

<sup>3</sup>USM/DERS/Centre National de l'Energie, des Sciences et des Techniques Nucléaires (CNESTEN), Rabat, Morocco.

<sup>4</sup>Laboratoire de la Matière Condensée et des Sciences Interdisciplinaires (LaMCSi), Mohammed V University of Rabat, Faculty of Sciences, B.P. 1014 Rabat, Morocco.

October 20, 2020

## Abstract

In this paper, we use the density functional theory (DFT) calculations under Quantum Espresso package to characterize the doping effect of sulfur substituting on the Zirconium dioxide ZrO<sub>2</sub>. Through the density of states and the band structure calculations, a direct band gap is appearing for the pure and doped studied system. The electronic properties analysis shows that the doping with sulfur could considerably decrease the band gap of doped ZrO<sub>2</sub> by the presence of an impurity state of sulfur 3 p on the up spin of the valence band. The results of the ab-initio density functional theory investigations show that the substitutional sulfur dopants incorporated into the Zirconium dioxide ZrO<sub>2</sub> drastically and affect the electronic structure of the studied material. In fact, the doping of Zirconium dioxide ZrO<sub>2</sub> with appropriate concentration values of sulfur leads to band gap values in the interval (1-2) eV. We recall that the band structure and density of states can improve among others: the energy gap of this doped ZrO<sub>2</sub> material. In fact, we have started from 1.3 eV for the pure ZrO<sub>2</sub> to reach 1.2 eV for 9% of sulfur doping. This last energy gap value is suitable for photovoltaic application.

## Doping effect of sulfur substituting on Zirconium dioxide ZrO<sub>2</sub>

**S. IDRISI<sup>1,\*</sup>, S. ZITI<sup>3</sup>, H. LABRIM<sup>2</sup> and L. BAHMAD<sup>1,\*</sup>**

<sup>1</sup> Laboratoire de la Matière Condensée et des Sciences Interdisciplinaires (LaMCSi), Mohammed V University of Rabat, Faculty of Sciences, B.P. 1014 Rabat, Morocco.

<sup>2</sup> USM/DERS/Centre National de l'Energie, des Sciences et des Techniques Nucléaires (CNESTEN), Rabat, Morocco.

<sup>3</sup> Intelligence Artificial and Security of Systems, Mohammed V University of Rabat, Faculty of Sciences, B.P. 1014 Rabat, Morocco.

**Abstract:** 11\*) Corresponding authors:*samiraidrissi2013@gmail.com* (S. I) ;*lahou2002@gmail.com* (L.B);

In this paper, we use the density functional theory (DFT) calculations under Quantum Espresso package to characterize the doping effect of sulfur substituting on the Zirconium dioxide ZrO<sub>2</sub>. Through the density of states and the band structure calculations, a direct band gap is appearing for the pure and doped studied system. The electronic properties analysis shows that the doping with sulfur could considerably decrease the band gap of doped ZrO<sub>2</sub> by the presence of an impurity state of sulfur 3 p on the up spin of the valence band.

The results of the ab-initio density functional theory investigations show that the substitutional sulfur dopants incorporated into the Zirconium dioxide  $\text{ZrO}_2$  drastically and affect the electronic structure of the studied material. In fact, the doping of Zirconium dioxide  $\text{ZrO}_2$  with appropriate concentration values of sulfur leads to band gap values in the interval (1-2) eV.

We recall that the band structure and density of states can improve among others: the energy gap of this doped  $\text{ZrO}_2$  material. In fact, we have started from 1.3 eV for the pure  $\text{ZrO}_2$  to reach 1.2 eV for 9% of sulfur doping. This last energy gap value is suitable for photovoltaic application.

**Keywords:** Zirconia  $\text{ZrO}_2$ ; Doping; Band gap; gradient generalized approximation (GGA); DFT method.

## Introduction

As an essential ceramic compound, zirconium dioxide ( $\text{ZrO}_2$ ) has attracted immense attention, because of its higher refractory, thermal and mechanical properties [1- 7]. For the applications of light solar cells, the nanotechnology has focused on enormous improvement in the procedure of semiconductor nano-materials [8-12]. Because of the low production cost [13, 14], the development of renewable energy resources have a large interest in prepared solar cell technology owing to high power conversion efficiency.

On the other hand, the metal oxide layers such as  $\text{Al}_2\text{O}_3$ ,  $\text{TiO}_2$ ,  $\text{SiO}_2$ ,  $\text{MgO}_2$ , and  $\text{ZrO}_2$  have been used to act as an energy barriers for restraining charge recombination [15-20]. In visible and near infrared region (NIR), the Zirconia dioxide material  $\text{ZrO}_2$  host possesses a high physical, chemical stability and optical transparency. The energy transfer from  $\text{ZrO}_2$  to rare earth ions has been proved by different doping ions such as Yb 3p, Er 3p, Tm 3p, Tb 3p, Eu 3p and Ho 3p [21-24]. In addition, the  $\text{ZrO}_2$  might be a good spectrum modifying matrix serving as a photon-conversion and an electron transporting layer. Therefore, the over coating of co-doped Yb-3p and Er-3p have the wide band gap value (4-6 eV) of the material  $\text{ZrO}_2$  [26-27]. The charge recombination participates to the loss of charge carriers and therefore decreases the photovoltaic performance of the cell [28-35].

Moreover, the several efforts on studying [36-38] have been devoted to the study of ferromagnetism tempted by the transition metal doping of semiconductor oxides  $\text{ZrO}_2$ , called diluted magnetic semiconductors (DMSs) [39-40]. Because of the ferromagnetism in semiconductor metal oxides discovers, main applications in spintronics and optoelectronics are achieved. However, it remains unclear whether ferromagnetism is an intrinsic property of the system or it is due to the combination of magnetic impurities [41, 42]. Also, the Oxides  $\text{ZrO}_2$  have been also predicted as ferromagnets at room temperature when doped by the light 2p elements (N) [43].

The aim of this work is to analyze and discuss the band gap values of the zirconium dioxide  $\text{ZrO}_2$  by doping this material with different concentrations of the sulfur element (S). In fact, the doping sulfur is an efficient method for narrowing the band gap energy of semiconductor oxide and shifts the threshold wavelength to the visible light region, see Refs. [44-45]. This could be helpful to use solar energy for the elimination of organic hazards by photocatalysis.

In the present study, the effect of doping this material has been discussed, as function of the different concentrations: doped  $\text{ZrO}_2$  with 5 %, 9 %, 14 % and 18% of sulfur. These concentrations are below the percolation threshold of the pure dioxide  $\text{ZrO}_2$  compound. For this purpose, we study such properties by using the DFT method under the Quantum Espresso package.

## Crystal structure and calculation method

In this paper, we are discussing the results of doping effect of Sulfur on Zirconium dioxide  $\text{ZrO}_2$ . The structure of the pure Zirconium dioxide  $\text{ZrO}_2$  as demonstrated in Fig. 1, by the Xcrysden package [46]. The  $\text{ZrO}_2$  has the cubic structure with the space group “Fm3m” (N° 225). The lattice constant is chosen to take the value 5.149 Å [47] and very near to the other theoretical studies 5.139 and 5.154 Å [48, 49]. The zirconium atoms are occupying (0, 0, 0) while the oxygen atoms reside in positions: (1/4, 1/4, 1/4) and (3/4, 3/4, 3/4).

To study the doping effect of sulfur substituting on the Zirconium dioxide  $\text{ZrO}_2$ . Through the density of states and the band structure calculations of the pure and doped zirconium dioxide  $\text{ZrO}_2$  with sulfur. We apply the Abinitio method using the Quantum Espresso code [50]. In fact, the obtained calculations are established based on the Density Functional Theory (DFT).

Indeed, we executed our simulations under the ultra-soft pseudo-potential method [51]. In these numerical calculations, we have used the gradient generalized approximation GGA founded on the parametrization given by Perdew et al. [52]. We use this approximation to treat the exchange correlation functional.

The valence electron configuration for Zirconium (Zr), oxygen (O) and sulfur (S) are: Zr (4d 5s), (2s 2p) and (3s 3p), respectively. The electrons were treated explicitly as valence states and expanded in plane-waves. In this work, the cutoff energy is equivalent to the separation of valence and core configurations, this value is found to be about 340 eV. The special points sampling integration, in the Brillouin zone, were employed using the Monkhorst–Pack method [53]. The convergence tolerance, in our simulations are fixed to  $10^{-6}$  eV/atom. Some of our recent works have been based on the DFT study and other methods of numerical simulations [54-57].

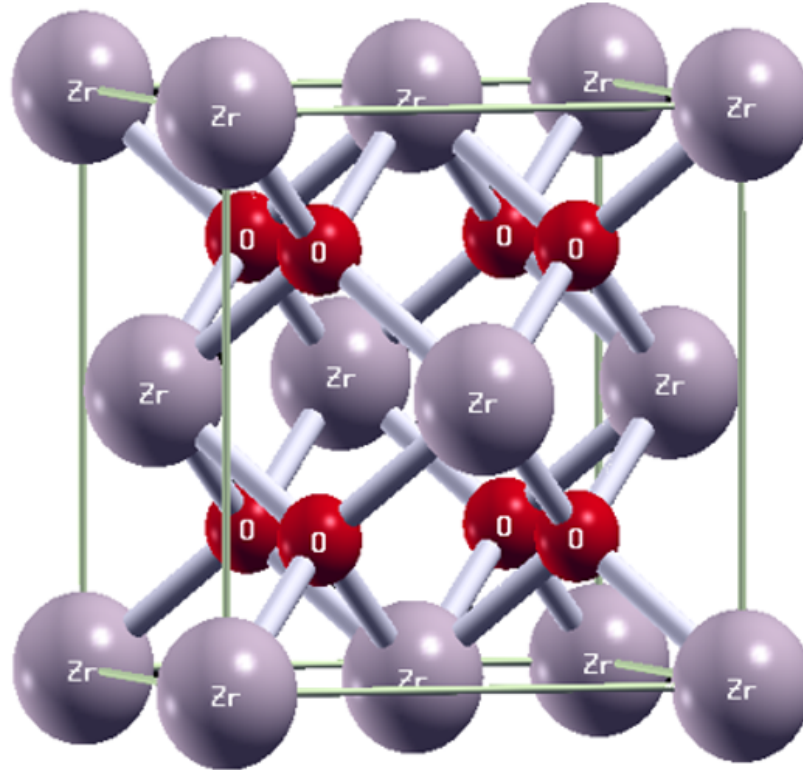


Fig.1: Schematic representation of the pure Zirconium dioxide  $\text{ZrO}_2$  using the Xcrysden package [46].

## Results and discussions

The total and partial density of states (DOS) of the pure zirconium dioxide  $\text{ZrO}_2$  have been plotted in order to explore the electronic behavior of the studied system.

The values of the electronegativity between the Zr and O elements are very different, while such values are: 1.33 for Zr atoms and 3.44 for O atoms. The difference between such values is equal to 2.11 which is larger than 1.7 on the Pauling scale. Additionally, the studied material is characterized by the ionic bonding. This ionic chemical bonding behavior can be explained by using the partial DOS from shown in Fig. 2 (a). From

this figure, the 2p orbitals of O and 4d of Zr are different below and above Fermi level. In fact, the 2p states of O dominate below the Fermi level, while in the above Fermi level, the 4 d states of Zr are dominating.

Moreover, Fig.2 (b) shows that this material does not present any magnetic behavior, since a perfect symmetry is present between up and down density of states. Also, this compound is a semiconductor with a direct band gap value [?] 3.1 eV. On the other hand, Fig.2 (c) presents the band structure of the pure ZrO<sub>2</sub>. This figure presents a direct band gap at the G point and confirms the value of the band gap of the pure ZrO<sub>2</sub> found in Figs.2 (a) and 2 (b).

Such results are in good agreement with other theoretical calculations such as the value 3.09 eV using VASP program [58] while for the monoclinic phase the obtained value is located between 3.4 and 5.4 eV using (SIESTA) package [59].

On the other hand, Figs. 3 (a), 3 (b) and 3 (c) provide the obtained results of doping the dioxide ZrO<sub>2</sub> with 5% of sulfur. In fact, Fig.3 (a) illustrates partial density of states showing the orbitals

Zr-(4d), O-(2p) and S-(3p). This figure shows also that the contribution of the partial density of states orbital O-(2p) is dominating in the valence band, while the contribution of the partial of density of states of Zr-(4d) is important in the conduction band region.

Moreover, Fig.3 (b) shows that the doping with 5% of sulfur make appearing a band gap value of 2.3 eV. Also, a perfect symmetry between spin-up and spin-down confirms the non-magnetic character of the doped zirconium dioxide ZrO<sub>2</sub>.

In addition, the band structure shown in Fig.3 (c) confirms the band gap value (2.3 eV) predicted in Figs.3 (a) and 3 (b). Similarly, to the Fig.2 (c), a direct band is found at the G point in Fig.3 (c).

Moreover, the existing experimental works showed that the formation of Zr–S bonds causes a decrease of the band gap from 3.38 eV to 2.46 eV [60]. When increasing the doping concentration values of sulfur atoms, the band gap decreases as it is shown Figs. 4 (a), 4 (b) and 4 (c). Such figures are plotted for 9% of sulfur concentration and predict a band gap value: 1.2 eV. This band gap decreases to achieve the value 0.6 eV as it is illustrated in Figs. 5 (a), 5 (b) and 5 (c) when doping with for 14% of sulfur. This band gap disappears when the doping concentration reaches value 18 % of the doping with sulfur as it is presented in Figs. 6 (a), 6 (b) and 6 (c).

Our results of band gap values of pure and doped zirconium dioxide ZrO<sub>2</sub> are summarized in table 1 for the concentration values: 5%, 9%, 14% and 18%. This table reproduces the already mentioned results from different figures.

To complete this study, we present in Fig.7 the energy and band gap of the doped ZrO<sub>2</sub> as a function of different concentrations (%) of sulfur atoms. From this figure, it is clear that when increasing the doping concentration of sulfur the band gap energy decreases. While the total energy of the studied system increases when increasing the sulfur concentration.

It is worth to note that the band gap value 1.2 eV, which useful for photovoltaic applications, which is reached for 9% of sulfur concentration.

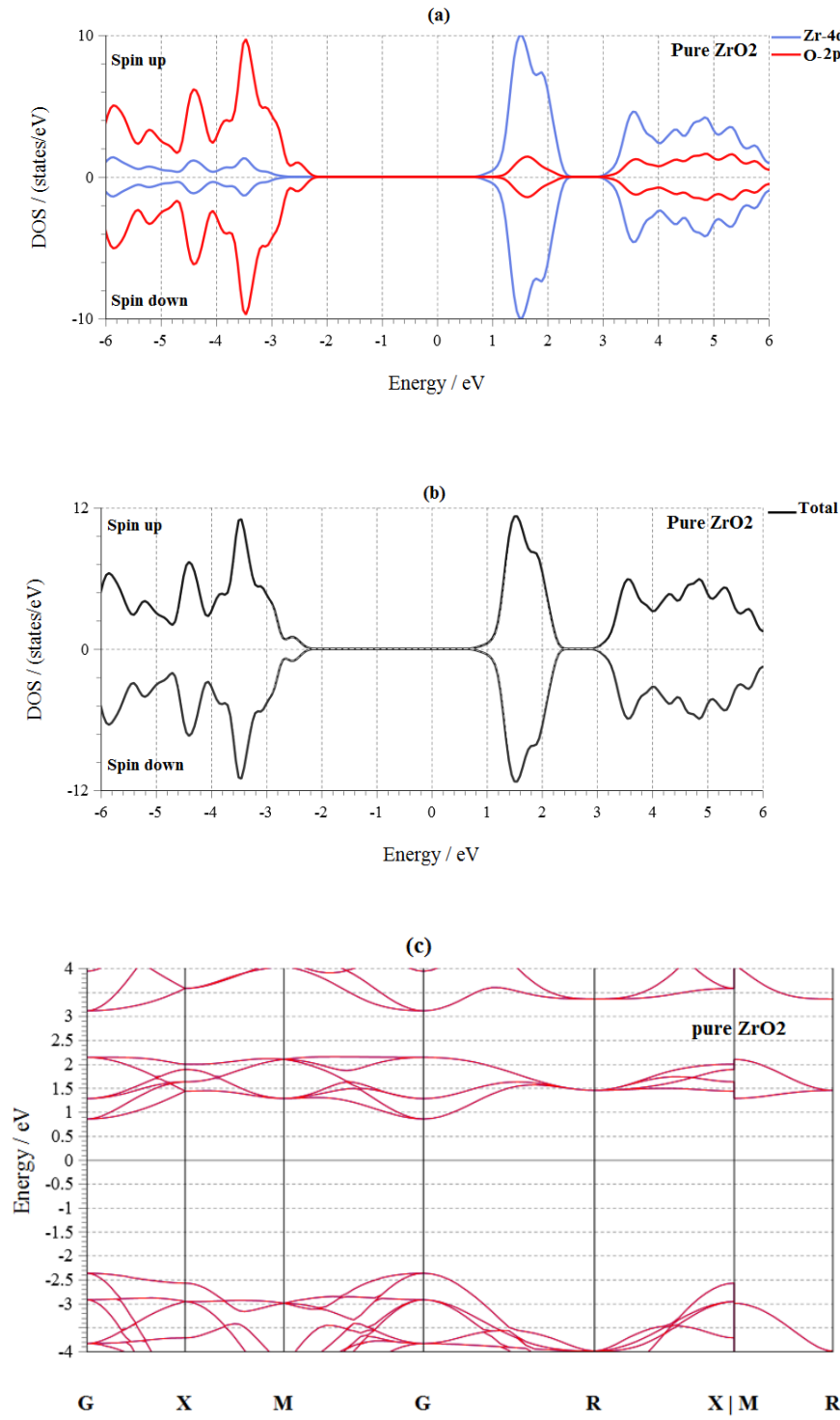


Fig.2: the pure ZrO<sub>2</sub>, partial density of states (DOS) in (a), Total DOS in (b) and Band structure in (c).

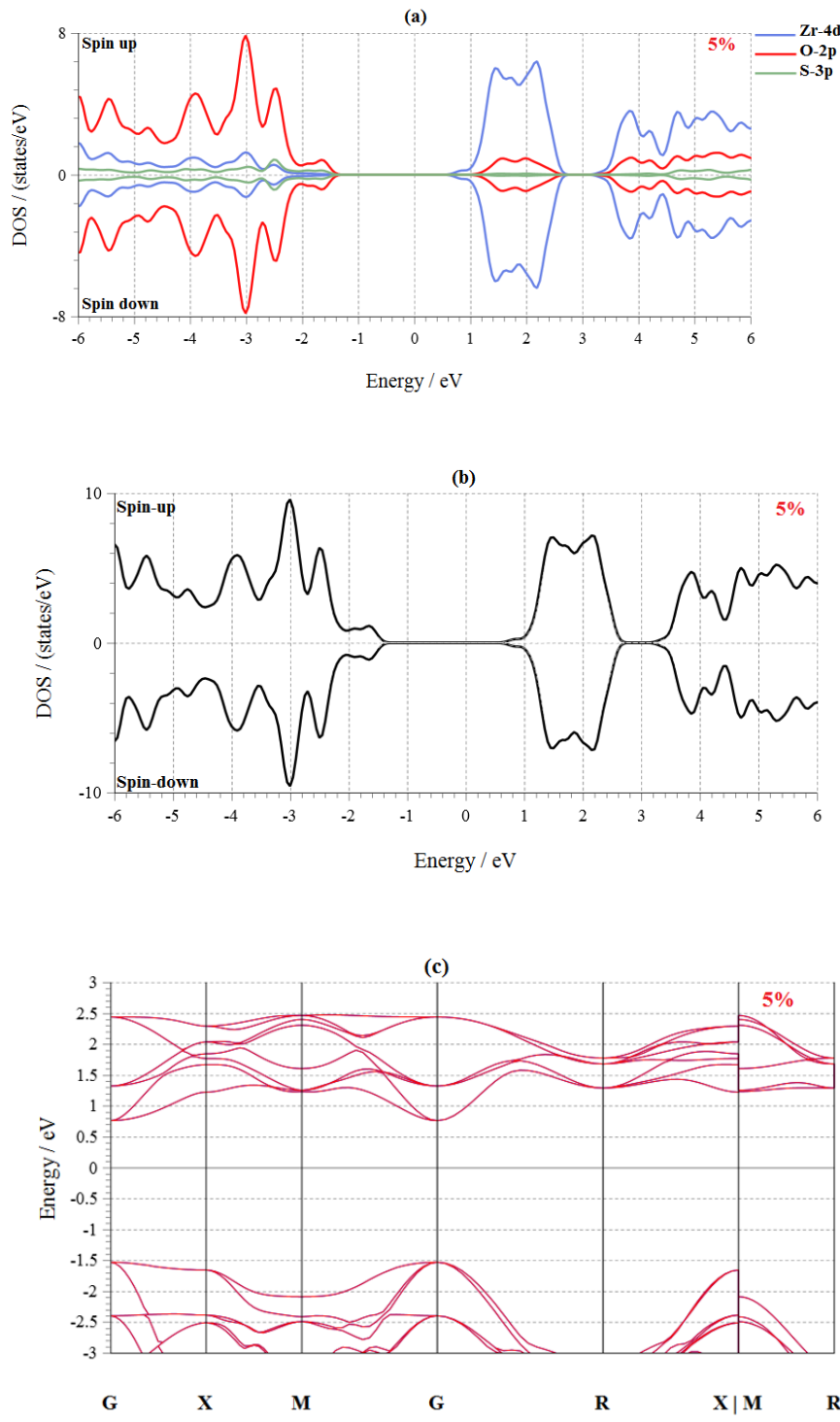


Fig.3: Doped ZrO<sub>2</sub> with 5% of Sulfur, partial density of states (DOS) in (a), Total DOS in (b) and Band structure in (c).

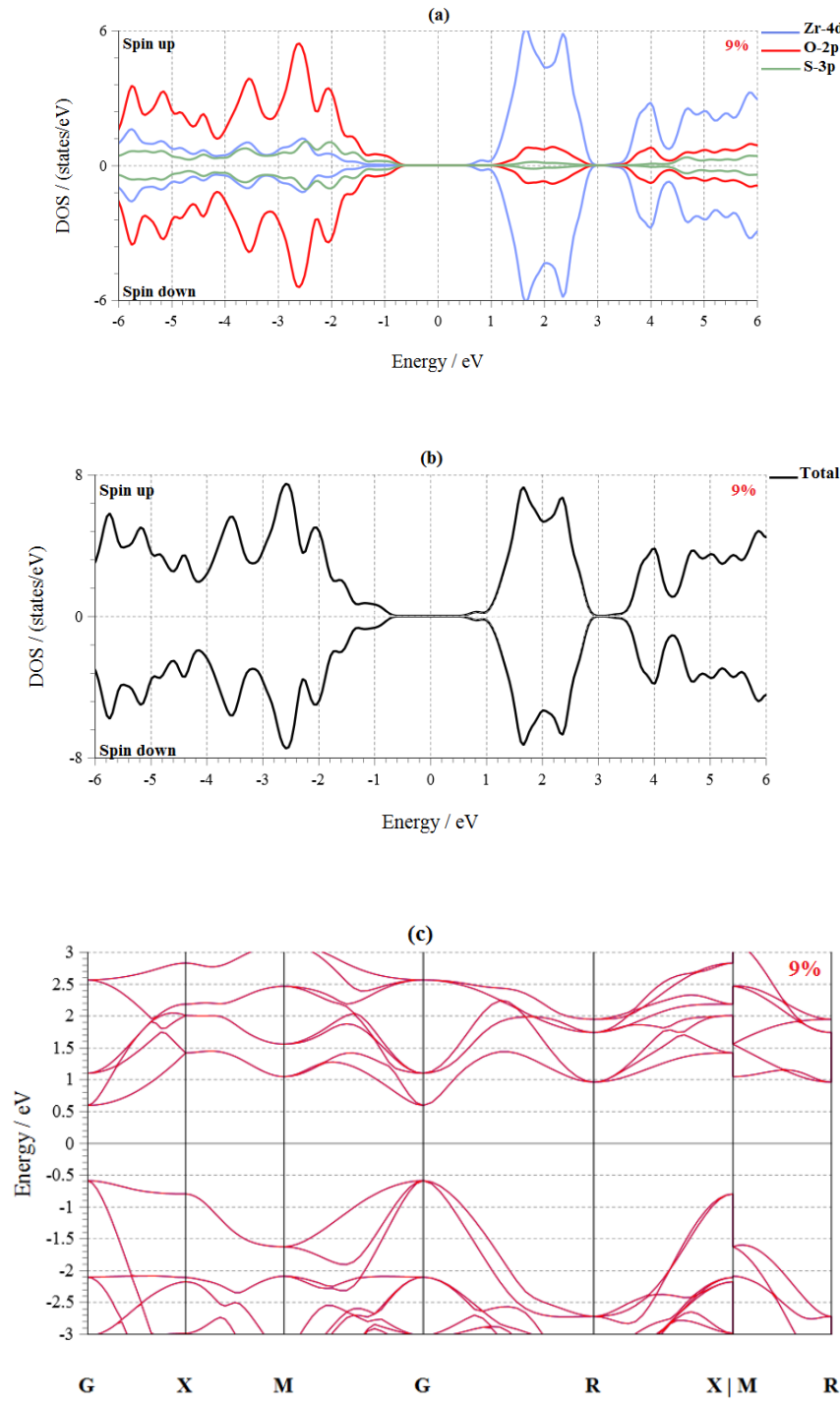


Fig.4: Doped ZrO<sub>2</sub> with 9% of Sulfur, partial density of states (DOS) in (a), Total DOS in (b) and Band structure in (c).

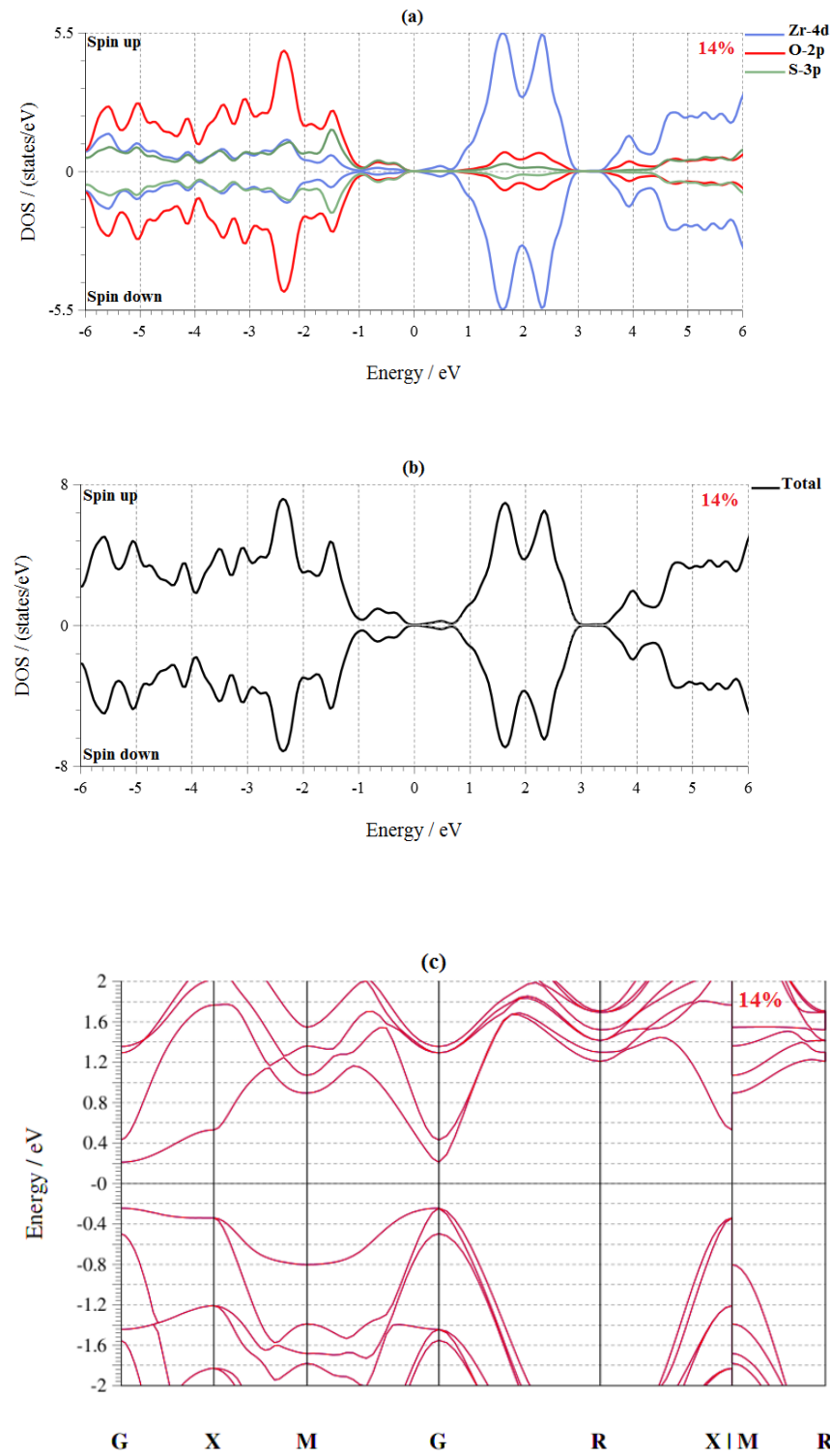


Fig.5: Doped ZrO<sub>2</sub> with 14% of Sulfur, partial density of states (DOS) in (a), Total DOS in (b) and Band structure in (c).

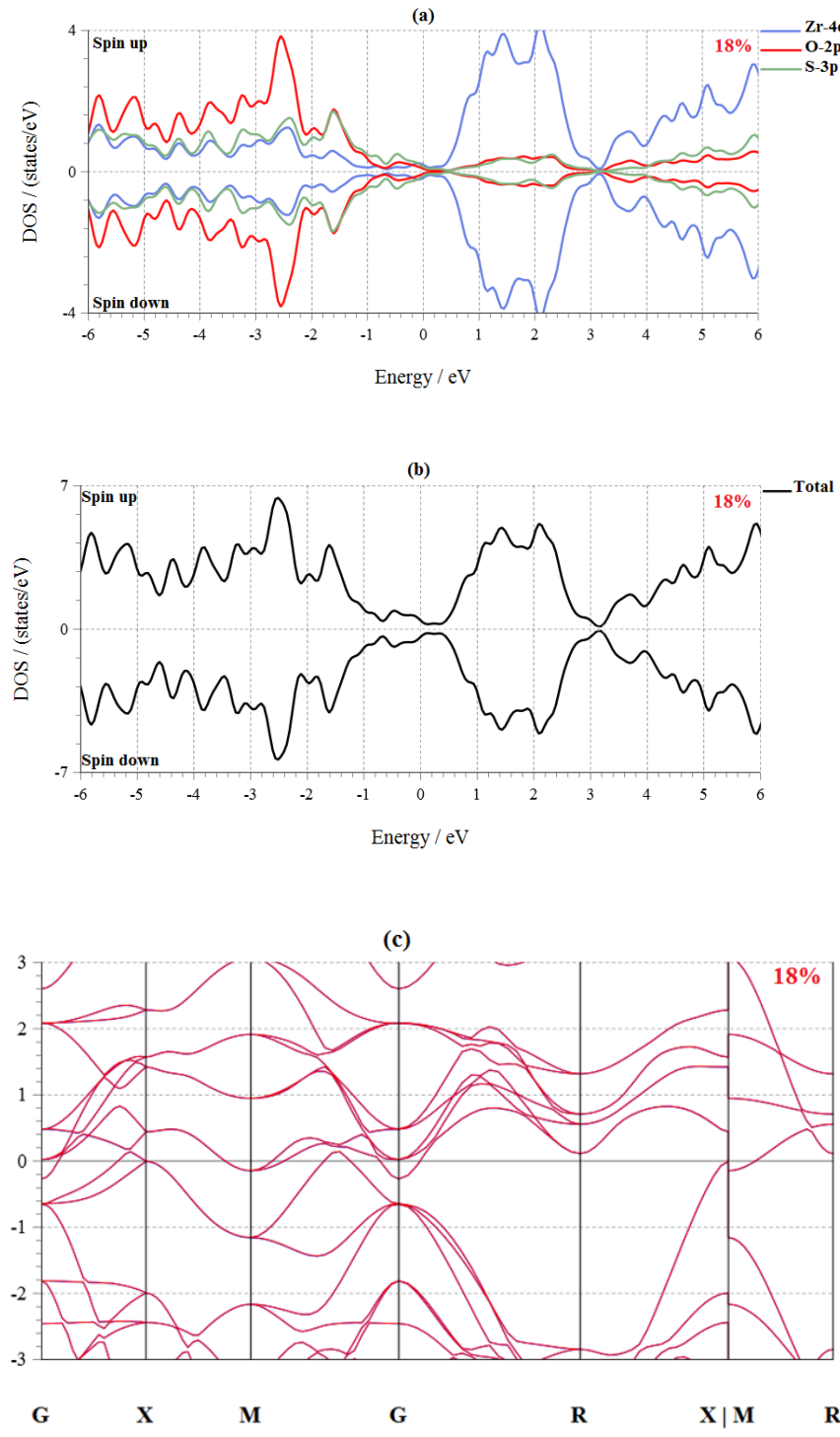


Fig.6: Doped ZrO<sub>2</sub> with 18% of Sulfur, partial density of states (DOS) in (a), Total DOS in (b) and Band structure in (c).

Fig.7: Energy and band gap of the doped ZrO<sub>2</sub> as a function of concentration (%) of impurities of sulfur.

Sulfur doped ZrO <sub>2</sub>	Eg (eV)
Pure case	3.1 present work 3.09 [58] 3.4 [59] 3.38 [60]
5 %	2.3
9 %	1.2
14 %	0.6
18 %	—

Table 1: Band gap values of the pure and doped zirconium dioxide ZrO<sub>2</sub>.

#### IV. Conclusion

In this paper, we have illustrated and discussed the effect of sulfur doping of the zirconium dioxide ZrO<sub>2</sub>. In fact, we have applied the gradient generalized approximation GGA. This material does not present any magnetic behavior, since a perfect symmetry is present between up and down density of states. Also, this pure material is a semiconductor with a direct band gap value 3.1 eV. The used concentrations of sulfur doping are: 5%, 9%, 14% and 18%. Such concentration values are below the percolation threshold. Moreover, the doping with 5% of sulfur make appear a band gap value of 2.3 eV. Such value is confirmed by the band structure diagrams. The obtained band gap value of 2.3 eV, when doping 5% of sulfur in this work is an agreement when doping ZrO<sub>2</sub> with experimental studies. We also deduce the band gap value 1.2 eV when doping this material with 9% of sulfur.

#### References:

- [1] Jie Chen, Zixin Weng, Yanru Tang, Xuezhan Yi, Yanna Tian, Di Zhao, Hui Lin, Shengming Zhou, Fabrication of ternary ZrO<sub>2</sub>-Al<sub>2</sub>O<sub>3</sub>-YAG:Ce ceramic phosphors for white light-emitting diodes, Journal of the European Ceramic Society, 2020, <https://doi.org/10.1016/j.jeurceramsoc.2020.10.027>.
- [2] Lida Heng, Jeong Su Kim, Juei-Feng Tu, Sang Don Mun, Fabrication of precision meso-scale diameter ZrO<sub>2</sub> ceramic bars using new magnetic pole designs in ultra-precision magnetic abrasive finishing, Ceramics International, Volume 46, Issue 11, Part A, 2020, Pages 17335-17346, <https://doi.org/10.1016/j.ceramint.2020.04.022>.
- [3] Jie Wu, Lin Chen, Yao Qu, Lei Dong, Jinliang Guo, Dejun Li, Wenbin Xue, In-situ high temperature electrochemical investigation of ZrO<sub>2</sub>/CrN ceramic composite film on zirconium alloy, Surface and Coatings Technology, Volume 359, 2019, Pages 366-373, <https://doi.org/10.1016/j.surfcoat.2018.12.093>.
- [4] Jun Yu, Feng-Xiu Yu, Shan Wang, Jie-Feng Zhang, Feng-Qiang Fan, Qiang Long, Effect of dispersant content and drying method on ZrO<sub>2</sub>@Al<sub>2</sub>O<sub>3</sub> multiphase ceramic powders, Ceramics International, Volume 44, Issue 15, 2018, Pages 17630-17634, <https://doi.org/10.1016/j.ceramint.2018.06.224>.
- [5] Yana Xia, Jun Mou, Guanyu Deng, Shanhong Wan, Kiet Tieu, Hongtao Zhu, Qi Xue, Sintered ZrO<sub>2</sub>-TiO<sub>2</sub> ceramic composite and its mechanical appraisal, Ceramics International, Volume 46, Issue 1, 2020, Pages 775-785, <https://doi.org/10.1016/j.ceramint.2019.09.032>.
- [6] Rana, S.; Fangueiro, R. Advanced Composite Materials for Aerospace Engineering: Processing, Properties and Applications; Wood head Publishing: Cambridge, UK, 2016.
- [7] Asl, M. S.; Nayebi, B.; Ahmadi, Z.; Zamharir, M.J.; Shokouhimehr, M. Effects of carbon additives on the properties of ZrB<sub>2</sub>-based composites: A review. Ceram. Int. 2018, 44, 7334–7348.
- [8] C. Dong, X. Li, J. Qi, First-principles investigation on electronic properties of quantum dot-sensitized solar cells based on anatase TiO<sub>2</sub> nanotubes, J. Phys. Chem. C 115 (2011) 20307e20315.
- [9] F.C. Krebs, S.A. Gevorgyan, J. Alstrup, A roll-to-roll process to flexible polymer solar cells: model studies, manufacture and operational stability studies, J. Mater. Chem. 19 (2009) 5442e5451.

- [10] M. Helgesen, R. Søndergaard, F.C. Krebs, Advanced materials and processes for polymer solar cell devices, *J. Mater. Chem.* 20 (2010) 36e60.
- [11] A. Cerdan-Pasaran, T. Lopez-Luke, D. Esparza, I. Zarazua, E. De la Rosa, R. Fuentes-Ramirez, A. Alatorre-Ordaz, A. Sanchez-Solis, A. Torres-Castro, J. Z. Zhang, Photovoltaic properties of multilayered quantum dot/quantum rod-sensitized TiO<sub>2</sub> solar cells fabricated by SILAR and electrophoresis, *Phys. Chem. Chem. Phys.* 17 (2015) 18590e18599.
- [12] D. Esparza, I. Zarazua, T. Lopez-Luke, A. Cerdan-Pasaran, A. Sanchez-Solís, A. Torres-Castro, I. Mora-Sero, E. De la Rosa, Effect of different sensitization technique on the photo conversion efficiency of CdS quantum dot and Cd Sequantum rod sensitized TiO<sub>2</sub>solar cells, *J. Phys. Chem. C* 119 (2015)13394e13403.
- [13] Yanxing Zhang, Zongxian Yang, The mechanism of the high resistance to sulfur poisoning of the rhenium doped nickel/yttria-stabilized zirconia, *Applied Surface Science*, Volume 447, 2018, Pages 561-568, <https://doi.org/10.1016/j.apsusc.2018.04.010>.
- [14] A. Yella, H. -W. Lee, H.N. Tsao, C. Yi, A. K. Chandiran, M. K. Nazeeruddin, Porphyrin-sensitized solar cells with cobalt (II/III)-based redox electrolyte exceed 12 percent efficiency, *Science* 334 (2011) 629e634
- [15] D. Komaraiah, E. Radha, J. Sivakumar, M.V. Ramana Reddy, R. Sayanna, Photoluminescence and photocatalytic activity of spin coated Ag+ doped anatase TiO<sub>2</sub> thin films, *Optical Materials*, Volume 108, 2020, 110401, <https://doi.org/10.1016/j.optmat.2020.110401>.
- [16] Sujubili Narzary, K. Alamelu, V. Raja, B.M. Jaffar Ali, Visible light active, magnetically retrievable Fe<sub>3</sub>O<sub>4</sub>@SiO<sub>2</sub>@g-C<sub>3</sub>N<sub>4</sub>/TiO<sub>2</sub> nanocomposite as efficient photocatalyst for removal of dye pollutants, *Journal of Environmental Chemical Engineering*, Volume 8, Issue 5, 2020, 104373, <https://doi.org/10.1016/j.jece.2020.104373>.
- [17] Z.F. Liu, M. Miyauchi, Y. Uemura, Y. Cui, K. Hara, Z.G. Zhao, K. Sunahara, A. Furube, Enhancing the performance of quantum dots sensitized solar cell by SiO<sub>2</sub> surface coating, *Appl. Phys. Lett.* 96 (2010) 233107.
- [18] Fabrice Kwefeu Mbakop, Ahmat Tom, Abdouramani Dadjé, Aloyem Kazé Claude Vidal, Noël Djongyang, One-dimensional comparison of TiO<sub>2</sub>/SiO<sub>2</sub> and Si/SiO<sub>2</sub> photonic crystals filters for thermophotovoltaic applications in visible and infrared, *Chinese Journal of Physics*, Volume 67, 2020, Pages 124-134, <https://doi.org/10.1016/j.cjph.2020.06.004>.
- [19] E. Barea, X.Q. Xu, V. Gonzalez-Pedro, T. Ripolles-Sanchis, F. Fabregat-Santiago,J. Bisquert, Origin of efficiency enhancement in Nb<sub>2</sub>O<sub>5</sub> coated titanium dioxide nano rod based dye sensitized solar cells, *Energy Environ. Sci.* 4 (2011)3414e3419.
- [20] J. Wang, T. Ming, Z. Jin, J. Wang, L.-D. Sun, C.-H. Yan, Photon energy up con-version through thermal radiation with the power efficiency reaching 16%, *Nat. Commun.* 5 (2014) 5669,<http://dx.doi.org/10.1038/ncomms6669>.
- [21] L.A. Diaz-Torres, P. Salas, C. Angeles-Chavez, O. Meza, T. Lopez-Luke, Greenup conversion emission dependence on size and surface residual contaminants in nano-crystalline ZrO<sub>2</sub>:Er<sub>3</sub>, *J. Sol-Gel Sci. Technol.* 63 (2012) 473e480.
- [22] L.A. Diaz-Torres, O. Meza, D. Solis, P. Salas, E. De la Rosa, Visible up conversion emission and non radiative direct Yb 3p to Er 3p energy transfer processes in nano-crystalline ZrO<sub>2</sub>:Yb<sub>3</sub>,Er<sub>3</sub>, *Opt. Laser Eng.* 49 (2011) 703e708.
- [23] V.H. Romero, E. De la Rosa, T. Lopez-luke, P. Salas, C. Angeles, Brilliant blue,green and orange-red emission band on Tm 3p,Tb 3p and Eu 3p doped ZrO<sub>2</sub> nanocrystals, *J. Phys. D. Appl. Phys.* 43 (2010) 465105 (8pp).

- [24] D. Solís, E. De la Rosa, P. Salas, C. Angeles-Chavez, Green up converted emission enhancement of ZrO<sub>2</sub>: Yb 3p -Ho 3p nanocrystals, *J. Phys. D. Appl. Phys.* 42 (2009) 235105 (8pp).
- [26] K. Zhao, Z.X. Pan, I. Mora-Sero, E. Canovas, H. Wang, Y. Song, X.Q. Gong, J. Wang, M. Bonn, J. Bisquert, X.H. Zhong, Boosting power conversion efficiencies of quantum-dot-sensitized solar cells beyond 8% by recombination control, *J. Am. Chem. Soc.* 137 (2015) 5602e5609.
- [27] D. Ramachari, D. Esparza, T. López-Luke, V.H. Romero, L. Perez-Mayen, E. De la Rosa, C.K. Jayasankar, Synthesis of co-doped Yb<sup>3+</sup>-Er<sup>3+</sup>:ZrO<sub>2</sub> up conversion nanoparticles and their applications in enhanced photovoltaic properties of quantum dot sensitized solar cells, *Journal of Alloys and Compounds*, Volume 698, 2017, Pages 433-441, <https://doi.org/10.1016/j.jallcom.2016.12.026>.
- [28] Albert Veved, Geh Wilson Ejuh, Noël Djongyang, Study of the optoelectronic and piezoelectric properties of ZrO<sub>2</sub> doped PVDF from quantum chemistry calculations, *Chinese Journal of Physics*, Volume 63, 2020, Pages 213-219, <https://doi.org/10.1016/j.cjph.2019.10.022>.
- [29] Yanyan Li, Li Zhao, Shoubin Wei, Meng Xiao, Binghai Dong, Li Wan, Shimin Wang, Effect of ZrO<sub>2</sub> film thickness on the photoelectric properties of mixed-cation perovskite solar cells, *Applied Surface Science*, Volume 439, 2018, Pages 506-515, <https://doi.org/10.1016/j.apsusc.2018.01.005>.
- [30] Mohammad Zarei, Sensitive visible light-driven photoelectrochemical aptasensor for detection of tetracycline using ZrO<sub>2</sub>/g-C<sub>3</sub>N<sub>4</sub> nanocomposite, *Sensors International*, Volume 1, 2020, 100029, <https://doi.org/10.1016/j.sintl.2020.100029>.
- [31] Ibrahim M.A. Mohamed, Van-Duong Dao, Ahmed S. Yasin, Hamouda M. Mousa, Mohamed A. Yassin, Muhammad Yasir Khan, Ho-Suk Choi, Nasser A.M. Barakat, Physicochemical and photoelectrochemical characterization of novel N-doped nanocomposite ZrO<sub>2</sub>/TiO<sub>2</sub> photoanode towards technology of dye-sensitized solar cells, *Materials Characterization*, Volume 127, 2017, Pages 357-364, <https://doi.org/10.1016/j.matchar.2017.03.014>.
- [32] Xiaojie Yang, Li Zhao, Kangle Lv, Binghai Dong, Shimin Wang, Enhanced efficiency for dye-sensitized solar cells with ZrO<sub>2</sub> as a barrier layer on TiO<sub>2</sub> nanofibers, *Applied Surface Science*, Volume 469, 2019, Pages 821-828, <https://doi.org/10.1016/j.apsusc.2018.10.242>.
- [33] Mohammad Zarei, Ultrasonic-assisted preparation of ZrO<sub>2</sub>/g-C<sub>3</sub>N<sub>4</sub> nanocomposites with high visible-light photocatalytic activity for degradation of 4-chlorophenol in water, *Water-Energy Nexus*, Volume 3, 2020, Pages 135-142, <https://doi.org/10.1016/j.wen.2020.08.002>.
- [34] Xiaojie Yang, Li Zhao, Kangle Lv, Binghai Dong, Shimin Wang, Enhanced efficiency for dye-sensitized solar cells with ZrO<sub>2</sub> as a barrier layer on TiO<sub>2</sub> nanofibers, *Applied Surface Science*, Volume 469, 2019, Pages 821-828, <https://doi.org/10.1016/j.apsusc.2018.10.242>.
- [35] Abdulmenan M. Hussein, Anastasiia V. Iefanova, Ranjit T. Koodali, Brian A. Logue, Rajesh V. Shende, Interconnected ZrO<sub>2</sub> doped ZnO/TiO<sub>2</sub> network photoanode for dye-sensitized solar cells, *Energy Reports*, Volume 4, 2018, Pages 56-64, <https://doi.org/10.1016/j.egyr.2018.01.007>.
- [36] Fert, A. Nobel Lecture: Origin, Development, and Future of Spintronic. *Rev. Mod. Phys.* 2008, 80, 1517-1529.
- [37] Rahman, M. A.; Rout, S.; Thomas, J. P.; McGillivray, D.; Leung, K. T. Defect-Rich Dopant-free ZrO<sub>2</sub> Nanostructures with Superior Dilute Ferromagnetic Semiconductor Properties. *J. Am. Chem. Soc.* 2016, 138, 11896-11906.
- [38] Chandragiri Venkata Reddy, I. Neelakanta Reddy, Bhargav Akkinepally, V.V.N. Harish, Kakarla Raghava Reddy, Shim Jaesool, Mn-doped ZrO<sub>2</sub> nanoparticles prepared by a template-free method for electrochemical energy storage and abatement of dye degradation, *Ceramics International*, Volume 45, Issue 12, 2019, Pages 15298-15306, <https://doi.org/10.1016/j.ceramint.2019.05.020>.

- [39] Zeitschrift fur Kristallographie - Crystalline Materials, Volume 232, Issue 1-3, Pages 161–183, eISSN 2196-7105, ISSN 2194-4946, DOI: <https://doi.org/10.1515/zkri-2016-1981>.
- [40] Zippel, J.; et al. Defect-Induced Ferromagnetism in Undoped and Mn-Doped Zirconia Thin Films. *Phys. Rev. B* 2010, 82, No. 125209.
- [41] Dietl, T. A Ten-year Perspective on Dilute Magnetic Semiconductors and Oxides. *Nat. Mater.* 2010, 9, 965–974.
- [42] Ogale, S. B. Dilute Doping, Defect, and Ferromagnetism in Metal Oxide Systems. *Adv. Mater.* 2010, 22, 3125–3155.
- [43] Zhu, H.; Li, J.; Chen, K.; Yi, X.; Cheng, S.; Gan, F. Nature of Charge Transport and p- electron Ferromagnetism in Nitrogen-doped ZrO<sub>2</sub>: An Ab-initio Perspective. *Sci. Rep.* 2015, 5, No. 8586.
- [44] T. Ohno, M. Akiyoshi, T. Umebayashi, K. Asai, T. Mitsui, M. MatsumuraPreparation of S-doped TiO<sub>2</sub> photocatalysts and their photocatalytic activities under visible light *Appl. Catal. A: Gen.*, 265 (2004), pp. 115-121
- [45] Lijing Zhang, Xiufang Zhu, Zhihui Wang, Shan Yun, Tan Guo, Jiadong Zhang, Tao Hu, Jinlong Jiang and Jing Chen [10.1039/C8RA07751G](https://doi.org/10.1039/C8RA07751G)(Paper) *RSC Adv.*, 2019, **9** , 4422-4427
- [46] A. Kokalj, XCrySDen-a new program for displaying crystalline structures and electron densities, *J. Mol. Graphics Modelling*, 1999, 17, 176–179.
- [47] D. A. WRIGHT, J. S. THORP, A. AYPAR, H. P. BUCKLEY; *JOURNAL OF MATERIALS SCIENCE* 8 (1973) 876-882.
- [48] J.C. Garcia, L.M.R. Scolfaro, A.T. Lino, V.N. Freire, G.A. Farias, C.C. Silva, H.W. Leite, Alves, S. C. P. Rodrigues, E.F. da Silva Jr., Structural, electronic, and optical properties of ZrO<sub>2</sub> from ab initio calculations, *J. Appl. Phys.* 100 (2006) 104103.
- [49] E.V. Stefanovich, A. Shluger, C.R. Catlow, Theoretical study of the stabilization of cubic- phase ZrO<sub>2</sub> by impurities, *Phys. Rev. B* 49 (1994) 11560.
- [50] P. Giannouzzi et al. *J. Phys.: Condens. Matter* 21, (2009), 395502; URL, “<http://www.Quantum-espresso.org>”.
- [51] D. Vanderbilt, Soft self-consistent pseudo-potentials in a generalized eigenvalue formalism, *Phys. Rev. B*, 41, (1990), 7892-7895.
- [52] J.P. Perdew, J.A. Chevary, S.H. Vosko, K.A. Jackson, M.R. Pederson, D.J. Singh, C. Fiolhais, *Phys. Rev. B* 46 (1992) 6671.
- [53] H.J. Monkhorst, J.D. Pack *Phys. Rev. B*, 13 (1976), p. 5188
- [54] S. Idrissi, H. Labrim, S. Ziti, L. Bahmad, Structural, electronic, magnetic properties and critical behavior of the equiatomic quaternary Heusler alloy CoFeTiSn, *Physics Letters A*, 2020, 126453,<https://doi.org/10.1016/j.physleta.2020.126453>.
- [55] Idrissi, S., Labrim, H., Ziti, S. et al. Investigation of the physical properties of the equiatomic quaternary Heusler alloy CoYCrZ (Z = Si and Ge): a DFT study. *Appl. Phys. A* 126, 190 (2020).<https://doi.org/10.1007/s00339-020-3354-6>
- [56] Idrissi, S., Labrim, H., Ziti, S. et al. Characterization of the Equiatomic Quaternary Heusler Alloy ZnCdRhMn: Structural, Electronic, and Magnetic Properties. *J Supercond Nov Magn* 33, 3087–3095 (2020).<https://doi.org/10.1007/s10948-020-05561-8>
- [57] S. Idrissi, S. Ziti, H. Labrim, L. Bahmad, Band gaps of the solar perovskites photovoltaic CsXCl<sub>3</sub> (X=Sn, Pb or Ge), *Materials Science in Semiconductor Processing*, Volume 122, 2021,

105484,<https://doi.org/10.1016/j.mssp.2020.105484>.

[58] Haoyuan Wang, Na Lin, Ran Xu, Yifei Yu, Xian Zhao, First principles studies of electronic, mechanical and optical properties of Cr-doped cubic ZrO<sub>2</sub>, Chemical Physics, Volume 539, 2020, 110972, <https://doi.org/10.1016/j.chemphys.2020.110972>.

[59] K. Seema, R. Kumar, Effect of dopant concentration on electronic and magnetic properties of transition metal-doped ZrO<sub>2</sub>, J. Supercond. Nov. Magnetism 28 (9) (2015) 2735e2742.

[60] Oleksandr I. Malyi, Zhong Chen, Guo Gang Shuband Ping Wu; J. Mater. Chem., 2011, 21, 12363